$\bar{B}^*_{u,d,s} \to D^*_{u,d,s} V\,(V = D^{*-}_{d,s}, K^{*-}, \rho^-)$ weak decays*

Qin Chang(常钦)[1,2;1)] Yunyun Zhang(张云云)[1] Xiaonan Li(李晓楠)[1,3]

[1]Institute of Particle and Nuclear Physics, Henan Normal University, Henan 453007, China
[2]School of physics and electronic technology, Liaoning Normal University, Liaoning 116029, China
[3]School of physics and electronic engineering, Anyang Normal University, Henan 455000, China

Abstract: Motivated by the rapid development of heavy flavor physics experiments, we study the tree-dominated nonleptonic $\bar{B}^*_{u,d,s} \to D^*_{u,d,s} V$ ($V = D^{*-}, D^{*-}_s, K^{*-}, \rho^-$) decays within the factorization approach. The relevant transition form factors are calculated by employing the covariant light-front quark model. Helicity amplitudes are calculated and analyzed in detail, and a very clear hierarchical structure $|H_{-0}| \approx 2|H_{00}| > |H_{0-}| \approx |H| > |H_{0+}| \approx |H_{++}|$ is presented. The branching fractions are computed and discussed. Numerically, the CKM-favored $\bar{B}^*_q \to D^*_q \rho^-$ and $D^*_q D^{*-}_s$ decays have relatively large branching fractions, $\gtrsim O(10^{-8})$, and could be observed by LHC and Belle-II experiments in the future.

Keywords: weak decay, light-front quark model, heavy flavor physics

PACS: 13.25.Hw, 12.39.-x, 12.15.-y **DOI:** 10.1088/1674-1137/43/10/103104

1 Introduction

The B meson weak decay plays an important role in testing the flavor dynamics of the standard model (SM), searching for the possible hints of new physics, and investigating the approaches of dealing with the hadronic matrix element. Experimentally, with the successful running of B factories, BaBar and Belle, many $B\bar{B}$ samples have been accumulated, which provide a fertile ground for the b-physics study. Owing to the ongoing LHCb experiment [1], many measurements of B meson decays are refined, and some new decay modes are observed. Moreover, the running SuperKEKB/Belle-II experiment also provides us with a lot of information about B meson decays [2]. Meanwhile, there are also a plenty of other b-flavored hadron events, such as Λ_b and B^* et al., that will be accumulated in the future, which may provide much more extensive space for b-physics research.

The B^* meson with the quantum number of $n^{2s+1}L_J = 1^3S_1$ and $J^P = 1^-$ is the vector ground state of the $(b\bar{q})$ system [3-7], and it can in principle play a similar role to the B meson. However, the B^* meson decay is dominated by the electromagnetic process $B^* \to B\gamma$, and its weak decay is too rare to be observed in previous heavy-flavor experiments. Fortunately, due to the rapid development of particle physics experiments in recent years, this situation can be improved by LHC and Belle-II experiments in the future [1, 2, 8]. For instance, the annual integrated luminosity of Belle-II is expected to reach up to ~13 ab^{-1}, and the B^* weak decays with branching fractions $> O(10^{-9})$ will hopefully be observed [2, 9]. Moreover, the LHC experiment will also provide significant experimental information for B^* weak decays due to the much larger beauty production cross-section of pp collision relative to the e^+e^- collision [10]. Therefore, theoretical studies of B^* weak decays are urgently required to provide some useful suggestions and references for relevant measurements.

Some theoretical studies on B^* weak decays have been recently conducted. In Ref. [11], the pure leptonic $B^*_s \to \ell\ell$ and $B^*_{u,c} \to l\nu$ decays are studied, and the detectability of LHC on these decays is analyzed in detail. These decays are revisited in Ref. [12] with the decay constant obtained via a relativistic potential model. In addition, the impact of $\bar{B}^*_{s,d} \to \mu\mu$ on $\bar{B}_{s,d} \to \mu\mu$ decays is discussed in Ref. [13], and the authors of Refs. [14–17] probe the signatures of physics beyond the SM through these decays. Some semileptonic B^* decays are evaluated within the framework of QCD sum rules [18–20], the Bauer-Stech-Wirbel model [21], and the Bethe-Salpeter method [22]. The effects of new physics are studied in a

Received 27 June 2019, Published online 9 September 2019

* Supported by the National Natural Science Foundation of China (11875122 and 11475055) and the Program for Innovative Research Team in University of Henan Province (19IRTSTHN018)

1) E-mail: changqin@htu.edu.cn

model- independent way in Ref. [23]. Some CKM-favored $\bar{B}_q^* \to D_q P$ and $D_q V$ decays are evaluated in the framework of naive factorization (NF) [9, 24], perturbative QCD (PQCD) [25], and QCD factorization (QCDF) [26, 27]. In this study, we focus our attention on the $\bar{B}_q^* \to D_q^* V$ ($V = D^{*-}, D_s^{*-}, K^{*-}, \rho^-$) decay modes.

Comparing $\bar{B}_q^* \to D_q P$ and $D_q V$ decays with the corresponding $\bar{B}_q \to D_q^* P$ and $D_q^* V$ decays, respectively, one can find a close relationship between them, as their main difference is $\bar{B}_q^* \to D_q$ vs. $\bar{B}_q \to D_q^*$ [9, 24], and their amplitudes are similar to each other. The $\bar{B}_q^* \to D_q^* V$ process, meanwhile, is a peculiar decay mode, and there is no correspondence from B decays. Comparing with $\bar{B}_q^* \to D_q P$ and $D_q V$ decays, the $\bar{B}_q^* \to D_q^* V$ decay is far more complicated, because it involves higher allowed helicity states of initial and final mesons contributing to the amplitude, which is worth careful study. In addition, the form factors of $\bar{B}_q^* \to D_q^*$ and $\bar{B}_q^* \to V$ transitions play an important role in estimating the amplitudes, however there is no available results that can be currently used. Thus, in this study, we calculate these form factors within the framework of a covariant light-front quark model (CLFQM).

Our paper is organized as follows. In Section 2, after a brief review of the theoretical framework, the helicity amplitudes of $\bar{B}_q^* \to D_q^* V$ decays are calculated in detail. In Section 3, the input parameters used in this work are given, particularly, the relevant form factors are calculated within the CLFQM. Subsequently, the numerical results and discussions for the $\bar{B}_q^* \to D_q^* V$ decays are presented. Finally, we provide our summary in Section 4.

2 Theoretical framework

The effective Hamiltonian responsible for nonleptonic $\bar{B}^*$ decays can be written as

$$\mathcal{H}_{\rm eff} = \frac{G_{\rm F}}{\sqrt{2}} \sum_{p,p'=u,c} \left[V_{pb} V_{p'q}^* \sum_{i=1}^{2} C_i(\mu) O_i(\mu) + V_{pb} V_{pq}^* \sum_{i=3}^{10} C_i(\mu) O_i(\mu) \right] + h.c., \quad (1)$$

where $G_{\rm F}$ is the Fermi coupling constant, $V_{pb} V_{p^{(\prime)}q}^*$ ($q = d, s$) is the product of Cabibbo-Kobayashi-Maskawa (CKM) matrix elements, $C_i(\mu)$ is the Wilson coefficient and can be calculated with the perturbation theory [28, 29], O_i is local four-quark operator, and its explicit form can be found in, for instance, Refs. [28, 29].

To obtain the decay amplitudes, we have to deal with the hadronic matrix elements of local operators, $\langle V_1 V_2 | O_i | B^* \rangle$, involved in the amplitude. A simple way for this purpose is the naive factorization (NF) scheme [30-34] based on the color transparency mechanism [35, 36]. Within the NF approach, the hadronic matrix element of $B^* \to V_1 V_2$ decay can be factorized as

$$H_{\lambda_1 \lambda_2}^{V_1 V_2} \equiv \langle V_1 V_2 | Q_i | B^* \rangle \simeq \langle V_2 | J_2 | 0 \rangle \langle V_1 | J_1 | B^* \rangle, \quad (2)$$

where the recoil vector meson that carries away the spectator quark from B^* meson is referred to as V_1, and the emission vector is referred to as V_2; $\lambda_{1(2)}$ is the helicity of $V_{1(2)}$ meson, and the helicity of initial B^* meson satisfies $\lambda_{B^*} = \lambda_1 - \lambda_2$. The two current matrix elements $\langle V_2 | J_2 | 0 \rangle$ and $\langle V_1 | J_1 | B^* \rangle$ in Eq. (2) can be further parameterized by the decay constant and form factors.

In the framework of NF, the non-factorizable contributions dominated by the hard gluon exchange are lost. To evaluate these QCD corrections to the matrix elements and reduce the scale-dependence, the QCDF approach is explored by BBNS [37, 38]. Despite this, the NF approach is employed in this study because of the following reasons: (i) in the framework of QCDF, the amplitude obtained through NF can be treated as the leading-order (LO) contribution of the QCDF result. For the $b \to c$ induced tree-dominated nonleptonic $B^{(*)}$ decays, compared with the LO contribution, the NLO and NNLO non-factorizable QCD corrections generally yield about 4% and 2% contributions [27, 38, 39], respectively. Therefore, for the $B^* \to D^* V$ decays studied here, the NF can provide relatively reliable predictions, and the small non-factorizable QCD correction is numerically trivial before these B^* decay modes are measured precisely. (ii) The QCDF approach is not suitable anymore for the case of the heavy emission meson [38], for instance, $\bar{B}^* \to D^* \bar{D}^*$ decays.

The decay constant and form factors are essential inputs for evaluating current matrix elements in Eq. (2). The former is defined as

$$\langle V_2(\epsilon_2, p_2) | \bar{q} \gamma^\mu q | 0 \rangle = f_{V_2} m_2 \epsilon_2^{*\mu}, \quad (3)$$

where m_2 and ϵ_2 denote the mass and the polarization vector of the V_2 meson, respectively. The form factors for $B^* \to V_1$ transition are defined by [40]

$$\langle V_1(\epsilon_1, p_1) | \bar{c} \gamma_\mu b | B^*(\epsilon, p) \rangle = \epsilon \cdot \epsilon_1^* \left[-P_\mu \tilde{V}_1(q^2) + q_\mu \tilde{V}_2(q^2) \right] + \frac{(\epsilon \cdot q)(\epsilon_1^* \cdot q)}{m_{B^*}^2 - m_1^2} \left[P_\mu \tilde{V}_3(q^2) - q_\mu \tilde{V}_4(q^2) \right] - (\epsilon \cdot q) \epsilon_{1\mu}^* \tilde{V}_5(q^2) + (\epsilon_1^* \cdot q) \epsilon_\mu \tilde{V}_6(q^2), \quad (4)$$

$$\langle V_1(\epsilon_1, p_1) | \bar{c} \gamma_\mu \gamma_5 b | B^*(\epsilon, p) \rangle = -{\rm i} \varepsilon_{\mu\nu\alpha\beta} \epsilon^\alpha \epsilon_1^{*\beta} \times \left[P^\nu \tilde{A}_1(q^2) - q^\nu \tilde{A}_2(q^2) \right] + \frac{2{\rm i}}{m_{B^*}^2 - m_1^2} \epsilon_{\mu\nu\alpha\beta} p^\alpha p_1^\beta \times \left[\epsilon^\nu (\epsilon_1^* \cdot q) \tilde{A}_3(q^2) - \epsilon_1^{*\nu} (\epsilon \cdot q) \tilde{A}_4(q^2) \right], \quad (5)$$

where $\epsilon_{0123} = -1$, $P = p + p_1$, $q = p - p_1 = p_2$, and $\epsilon_{(1)}$ is the polarization vector of the $B^*(V_1)$ meson.

Subsequently, after contracting the current matrix elements, we can obtain the $H^{V_1V_2}_{\lambda_1\lambda_2}$ for the seven allowed helicity states of final mesons, written as

$$H^{V_1V_2}_{00} = f_{V_2} m_2 \left[\frac{p_c(m^2_{B^*}+m^2_1-m^2_2)}{m_1 m_2}\tilde{V}_1 + \frac{2m^2_{B^*}p^3_c}{(m^2_{B^*}-m^2_1)m_1m_2}\tilde{V}_3 - \frac{p_c(m^2_{B^*}-m^2_1-m^2_2)}{2m_1m_2}\tilde{V}_5 + \frac{p_c(m^2_{B^*}-m^2_1+m^2_2)}{2m_1m_2}\tilde{V}_6 \right], \tag{6}$$

$$H^{V_1V_2}_{++} = f_{V_2} m_2 \left[\frac{3m^2_{B^*}+m^2_1-m^2_2}{2m_{B^*}}\tilde{A}_1 - \frac{m^2_{B^*}-m^2_1+m^2_2}{2m_{B^*}}\tilde{A}_2 + \frac{2p^2_c m_{B^*}}{m^2_{B^*}-m^2_1}\tilde{A}_4 - p_c\tilde{V}_5 \right], \tag{7}$$

$$H^{V_1V_2}_{--} = f_{V_2} m_2 \left[-\frac{3m^2_{B^*}+m^2_1-m^2_2}{2m_{B^*}}\tilde{A}_1 + \frac{m^2_{B^*}-m^2_1+m^2_2}{2m_{B^*}}\tilde{A}_2 - \frac{2p^2_c m_{B^*}}{m^2_{B^*}-m^2_1}\tilde{A}_4 - p_c\tilde{V}_5 \right], \tag{8}$$

$$H^{V_1V_2}_{+0} = f_{V_2} m_2 \left[-\frac{m^2_{B^*}-m^2_1}{m_2}\tilde{A}_1 + m_2\tilde{A}_2 + \frac{2m_{B^*}p_c}{m_2}\tilde{V}_1 \right], \tag{9}$$

$$H^{V_1V_2}_{-0} = f_{V_2} m_2 \left[\frac{m^2_{B^*}-m^2_1}{m_2}\tilde{A}_1 - m_2\tilde{A}_2 + \frac{2m_{B^*}p_c}{m_2}\tilde{V}_1 \right], \tag{10}$$

$$H^{V_1V_2}_{0-} = f_{V_2} m_2 \left[-\frac{m^2_{B^*}+3m^2_1-m^2_2}{2m_1}\tilde{A}_1 + \frac{m^2_{B^*}-m^2_1-m^2_2}{2m_1}\tilde{A}_2 - \frac{2p^2_c m^2_{B^*}}{(m^2_{B^*}-m^2_1)m_1}\tilde{A}_3 - \frac{p_c m_{B^*}}{m_1}\tilde{V}_6 \right], \tag{11}$$

$$H^{V_1V_2}_{0+} = f_{V_2} m_2 \left[\frac{m^2_{B^*}+3m^2_1-m^2_2}{2m_1}\tilde{A}_1 - \frac{m^2_{B^*}-m^2_1-m^2_2}{2m_1}\tilde{A}_2 + \frac{2p^2_c m^2_{B^*}}{(m^2_{B^*}-m^2_1)m_1}\tilde{A}_3 - \frac{p_c m_{B^*}}{m_1}\tilde{V}_6 \right], \tag{12}$$

where $p_c = \dfrac{\sqrt{[m^2_{B^*}-(m_1+m_2)^2][m^2_{B^*}-(m_1-m_2)^2]}}{2m_{B^*}}$.

Using the formulas given above, we can finally obtain helicity amplitudes of tree-dominated $\bar{B}^*_{u,d,s} \to D^*_{u,d,s}V$ ($V = D^{*-}, D^{*-}_s, K^{*-}, \rho^-$) decays, which can be written as

$$\mathcal{A}(B^{*-} \to D^{*0}K^{*-}) = \frac{G_F}{\sqrt{2}}[H^{D^*K^*}_{\lambda_{D^*}\lambda_{K^*}} V_{cb}V^*_{us}\alpha_1 + H^{K^*D^*}_{\lambda_{K^*}\lambda_{D^*}} V_{cb}V^*_{us}\alpha_2], \tag{13}$$

$$\mathcal{A}(B^{*-} \to D^{*0}\rho^-) = \frac{G_F}{\sqrt{2}}[H^{D^*\rho}_{\lambda_{D^*}\lambda_\rho} V_{cb}V^*_{ud}\alpha_1 + H^{\rho D^*}_{\lambda_\rho\lambda_{D^*}} V_{cb}V^*_{ud}\alpha_2], \tag{14}$$

$$\mathcal{A}(B^{*-} \to D^{*0}D^{*-}) = \frac{G_F}{\sqrt{2}}H^{D^{*0}D^{*-}}_{\lambda_{D^{*0}}\lambda_{D^{*-}}}[V_{cb}V^*_{cd}(\alpha_1+\alpha_4 + \alpha_{4,EW}) + V_{ub}V^*_{ud}(\alpha_4+\alpha_{4,EW})], \tag{15}$$

$$\mathcal{A}(B^{*-} \to D^{*0}D^{*-}_s) = \frac{G_F}{\sqrt{2}}H^{D^*D^*_s}_{\lambda_{D^*}\lambda_{D^*_s}}[V_{cb}V^*_{cs}(\alpha_1+\alpha_4+\alpha_{4,EW}) + V_{ub}V^*_{us}(\alpha_4+\alpha_{4,EW})], \tag{16}$$

$$\mathcal{A}(\bar{B}^{*0} \to D^{*+}K^{*-}) = \frac{G_F}{\sqrt{2}}H^{D^*K^*}_{\lambda_{D^*}\lambda_{K^*}} V_{cb}V^*_{us}\alpha_1, \tag{17}$$

$$\mathcal{A}(\bar{B}^{*0} \to D^{*+}\rho^-) = \frac{G_F}{\sqrt{2}}H^{D^*\rho}_{\lambda_{D^*}\lambda_\rho} V_{cb}V^*_{ud}\alpha_1, \tag{18}$$

$$\mathcal{A}(\bar{B}^{*0} \to D^{*+}D^{*-}) = \frac{G_F}{\sqrt{2}}H^{D^{*+}D^{*-}}_{\lambda_{D^{*+}}\lambda_{D^{*-}}}[V_{cb}V^*_{cd}(\alpha_1+\alpha_4+\alpha_{4,EW}) + V_{ub}V^*_{ud}(\alpha_4+\alpha_{4,EW})], \tag{19}$$

$$\mathcal{A}(\bar{B}^{*0} \to D^{*+}D^{*-}_s) = \frac{G_F}{\sqrt{2}}H^{D^*D^*_s}_{\lambda_{D^*}\lambda_{D^*_s}}[V_{cb}V^*_{cs}(\alpha_1+\alpha_4+\alpha_{4,EW}) + V_{ub}V^*_{us}(\alpha_4+\alpha_{4,EW})], \tag{20}$$

$$\mathcal{A}(\bar{B}^{*0}_s \to D^{*+}_s K^{*-}) = \frac{G_F}{\sqrt{2}}H^{D^*_sK^*}_{\lambda_{D^*_s K^*}} V_{cb}V^*_{us}\alpha_1, \tag{21}$$

$$\mathcal{A}(\bar{B}^{*0}_s \to D^{*+}_s\rho^-) = \frac{G_F}{\sqrt{2}}H^{D^*_s\rho}_{\lambda_{D^*_s}\lambda_\rho} V_{cb}V^*_{ud}\alpha_1, \tag{22}$$

$$\mathcal{A}(\bar{B}^{*0}_s \to D^{*+}_s D^{*-}) = \frac{G_F}{\sqrt{2}}H^{D^*_sD^*}_{\lambda_{D^*_s}\lambda_{D^*}}[V_{cb}V^*_{cd}(\alpha_1+\alpha_4+\alpha_{4,EW}) + V_{ub}V^*_{ud}(\alpha_4+\alpha_{4,EW})], \tag{23}$$

$$\mathcal{A}(\bar{B}^{*0}_s \to D^{*+}_s D^{*-}_s) = \frac{G_F}{\sqrt{2}}H^{D^{*+}_sD^{*-}_s}_{\lambda_{D^{*+}_s}\lambda_{D^{*-}_s}}[V_{cb}V^*_{cs}(\alpha_1+\alpha_4+\alpha_{4,EW}) + V_{ub}V^*_{us}(\alpha_4+\alpha_{4,EW})], \tag{24}$$

where $\alpha_1 = C_1 + \dfrac{C_2}{N_c}$, $\alpha_2 = C_2 + \dfrac{C_1}{N_c}$, $\alpha_4 = C_4 + v\dfrac{C_3}{N_c}$ and $\alpha_{4,EW} = C_{10} + \dfrac{C_9}{N_c}$ are effective coefficients, and $N_c = 3$ denotes the number of colors.

Using the helicity amplitudes given above, one can further obtain the branching fraction of $B^* \to D^*V$ decay, defined as

$$\mathcal{B}(B^* \to D^*V) = \frac{1}{3}\frac{1}{8\pi}\frac{p_c}{m^2_{B^*}\Gamma_{\rm tot}(B^*)}\sum_{\lambda_{B^*}\lambda_{D^*}\lambda_V}|A(B^* \to D^*V)|^2, \tag{25}$$

where $\Gamma_{\rm tot}(B^*)$ is the total decay width of B^* meson, and the factor 1/3 is caused by averaging over the spins of the initial state.

3 Numerical results and discussions

Using the theoretical formulas provided in the last section, we present our numerical evaluation and discussions. First, we would like to clarify the values of inputs used in our numerical calculation. For the well-known Fermi coupling constant G_F and the masses of mesons, we take their central values given by PDG [3]. For the CKM matrix elements, we adopt the Wolfenstein parameterization, and the four parameters A, λ, ρ and η are as follows [3]

$$A = 0.836^{+0.015}_{-0.015}, \quad \lambda = 0.22453^{+0.00044}_{-0.00044}, \quad \bar{\rho} = 0.122^{+0.018}_{-0.017}, \quad \bar{\eta} = 0.355^{+0.012}_{-0.011}. \tag{26}$$

Using these inputs, we can easily obtain the values of CKM elements relevant to this work, $V_{ud} = 0.97448^{+0.00010}_{-0.00010}$, $V_{us} = 0.22453^{+0.00044}_{-0.00044}$, $V_{ub} = 0.00122^{+0.00018}_{-0.00017} - i0.00354^{+0.00014}_{-0.00013}$, $V_{cd} = -0.22438^{+0.00044}_{-0.00044} - i0.00015^{+0.00001}_{-0.00001}$, $V_{cs} = 0.97359^{+0.00010}_{-0.00010}$, and $V_{cb} = 0.04215^{+0.00077}_{-0.00077}$ at the level of $O(\lambda^5)$. For the decay constants of emission mesons, we assume their values extracted from experimental data and predicted by lattice QCD

$$f_{D^*} = 223.5 \pm 8.4\,\text{MeV [41]}, \quad f_{D_s^*} = 268.8 \pm 6.6\,\text{MeV [41]}, \quad f_{K^*} = 204 \pm 7\,\text{MeV [42]}, \quad f_\rho = 210 \pm 4\,\text{MeV [43]}. \tag{27}$$

The total decay width of the B^* meson represents the essential input for evaluating the branching fraction, however, there is currently no available experimental result. Based on the fact that the radiative process $B^* \to B\gamma$ dominates the decays of the B^* meson [3], we can take the approximation that $\Gamma_{\rm tot}(B^*) \simeq \Gamma(B^* \to B\gamma)$. The predictions for $\Gamma(B^* \to B\gamma)$ have been obtained in various theoretical models [44-50]. In this study, the light-front quark model (LFQM) is employed to evaluate $\Gamma(B^* \to B\gamma)$. The relevant theoretical formulas have been obtained in Ref. [49]. Using the values of the Gaussian parameter β given in Refs. [51, 52], we can obtain the updated LFQM predictions for $\Gamma(B^* \to B\gamma)$ as follows

$$\Gamma_{\rm tot}(B^{*-}) \simeq \Gamma(B^{*-} \to B^-\gamma) = (349 \pm 18)\,\text{eV}, \tag{28}$$

$$\Gamma_{\rm tot}(\bar{B}^{*0}) \simeq \Gamma(\bar{B}^{*0} \to \bar{B}^0\gamma) = (116 \pm 6)\,\text{eV}, \tag{29}$$

$$\Gamma_{\rm tot}(\bar{B}_s^*) \simeq \Gamma(\bar{B}_s^* \to \bar{B}_s\gamma) = (84^{+11}_{-9})\,\text{eV}, \tag{30}$$

which agree with the ones obtained in previous works [44-50].

Besides the input parameters given above, the transition form factors $\tilde{V}_{1-6}^{B^*\to V_1}(m_2^2)$, $\tilde{A}_{1-4}^{B^*\to V_1}(m_2^2)$ are also essential ingredients for the estimation of certain nonleptonic B^* decay. However, there is currently no available result. In this work, we adopt the CLFQM [53–55] to evaluate their values. Our theoretical results for $\tilde{V}_{1-6}(q^2)$ and $\tilde{A}_{1-4}(q^2)$ defined by Eqs. (4) and (5) are given explicitly in the appendix. The convenient Drell-Tan-West frame, $q^+ = 0$, is used in the CLFQM [53–55]. This implies that the form factors are known only for space-like momentum transfer, because $q^2 = -q_\perp^2 \leqslant 0$, using the formulas given in the appendix. Meanwhile, the ones in the time-like region need an additional q^2 extrapolation. The momentum dependences of form factors in the space-like region can be efficiently parameterized and reproduced via the three parameter form (dipole approximation),

$$F(q^2) = \frac{F(0)}{1 - a(q^2/m_{B^*}^2) + b(q^2/m_{B^*}^2)^2}, \tag{31}$$

where, $F = \tilde{V}_{1-6}$ and $\tilde{A}_{1-4}$. The parameters a, b, and $F(0)$ can be first determined in the space-like region. Subsequently, we employ these results to evaluate $F(q^2)$ at $q^2 \geqslant 0$ via Eq. (31). Using the best-fit values of constituent quark masses and Gaussian parameter obtained in Refs. [51, 52], we provide our numerical results for the form factors of $B^* \to (D^*, K^*, \rho)$ and $B_s^* \to D_s^*$ transitions in Table 1. In the following numerical calculation, these values and their 10% are treated as default inputs and uncertainties, respectively.

Using theoretical formulas given in the last section and the inputs given above, we present our predictions for the branching fractions of $\bar{B}_q^* \to D_q^* V$ decays in Table 2, where the first theoretical error is caused by the uncertainties of CKM parameters, decay constants, and total

Table 1. Form factors of $B^* \to (D^*, K^*, \rho)$ and $B_s^* \to D_s^*$ transitions in CLFQM.

	$F^{B^*\to D^*}(0)$	a	b	$F^{B^*\to K^*}(0)$	a	b	$F^{B^*\to\rho}(0)$	a	b	$F^{B_s^*\to D_s^*}(0)$	a	b
$\tilde{A}_1$	0.66	1.31	0.42	0.33	1.75	0.89	0.27	1.79	0.97	0.65	1.42	0.64
$\tilde{A}_2$	0.35	1.32	0.42	0.27	1.75	0.88	0.25	1.80	0.97	0.38	1.47	0.67
$\tilde{A}_3$	0.07	1.79	1.10	0.07	2.28	2.20	0.07	2.39	2.37	0.10	1.89	1.33
$\tilde{A}_4$	0.08	1.81	1.15	0.07	2.29	2.33	0.06	2.35	2.46	0.09	1.88	1.36
$\tilde{V}_1$	0.67	1.31	0.43	0.33	1.74	0.96	0.28	1.79	0.01	0.66	1.43	0.64
$\tilde{V}_2$	0.36	1.32	0.42	0.27	1.74	0.95	0.25	1.80	1.02	0.38	1.48	0.67
$\tilde{V}_3$	0.13	1.72	1.01	0.11	2.16	2.04	0.11	2.23	2.16	0.15	1.79	1.20
$\tilde{V}_4$	0.00	–0.08	1.24	–0.01	2.91	4.24	–0.03	2.77	3.74	–0.02	2.22	1.92
$\tilde{V}_5$	1.17	1.30	0.40	0.68	1.71	0.90	0.60	1.76	0.95	1.19	1.41	0.61
$\tilde{V}_6$	0.48	1.29	0.40	0.16	1.67	0.81	0.14	1.70	0.82	0.53	1.35	0.56

Table 2. Branching fractions and helicity fractions (%) of $\bar{B}_q^* \to D_q^* V$ decays.

Decay mode	$\mathcal{B}$	f_{00}	f_{--}	f_{++}	f_{-0}	f_{+0}	f_{0-}	f_{0+}
$B^{*-} \to D^{*0} K^{*-}$	$1.10^{+0.01+0.19}_{-0.01-0.17} \times 10^{-9}$	24.4	4.5	0.3	69.2	0.0	1.4	0.2
$B^{*-} \to D^{*0} \rho^{-}$	$2.23^{+0.04+0.39}_{-0.04-0.35} \times 10^{-8}$	24.1	3.3	0.2	71.0	0.0	1.2	0.2
$B^{*-} \to D^{*0} D^{*-}$	$1.44^{+0.11+0.24}_{-0.11-0.22} \times 10^{-9}$	12.9	13.1	1.8	56.6	0.4	13.8	1.5
$B^{*-} \to D^{*0} D_s^{*-}$	$3.71^{+0.18+0.64}_{-0.18-0.57} \times 10^{-8}$	12.1	14.1	2.0	54.8	0.5	14.7	1.8
$\bar{B}^{*0} \to D^{*+} K^{*-}$	$3.40^{+0.24+0.58}_{-0.23-0.52} \times 10^{-9}$	19.7	3.2	0.3	73.2	0.0	3.4	0.2
$\bar{B}^{*0} \to D^{*+} \rho^{-}$	$6.85^{+0.26+1.17}_{-0.26-1.05} \times 10^{-8}$	20.1	2.5	0.2	74.4	0.0	2.6	0.2
$\bar{B}^{*0} \to D^{*+} D^{*-}$	$4.33^{+0.33+0.74}_{-0.32-0.66} \times 10^{-9}$	12.9	13.1	1.8	56.6	0.4	13.8	1.5
$\bar{B}^{*0} \to D^{*+} D_s^{*-}$	$1.11^{+0.06+0.19}_{-0.05-0.17} \times 10^{-7}$	12.1	14.1	2.0	54.8	0.5	14.7	1.8
$\bar{B}_s^{*0} \to D_s^{*+} K^{*-}$	$4.80^{+0.34+0.83}_{-0.32-0.74} \times 10^{-9}$	20.2	3.2	0.3	72.7	0.0	3.5	0.2
$\bar{B}_s^{*0} \to D_s^{*+} \rho^{-}$	$9.39^{+0.36+1.63}_{-0.35-1.46} \times 10^{-8}$	20.4	2.5	0.2	74.1	0.0	2.7	0.2
$\bar{B}_s^{*0} \to D_s^{*+} D^{*-}$	$6.10^{+0.47+1.03}_{-0.45-0.92} \times 10^{-9}$	13.3	13.0	1.7	56.2	0.3	14.1	1.4
$\bar{B}_s^{*0} \to D_s^{*+} D_s^{*-}$	$1.54^{+0.08+0.26}_{-0.07-0.24} \times 10^{-7}$	12.9	13.9	1.9	54.4	0.4	15.1	1.5

decay width. The second theoretical error, in turn, is caused by the form factors. Moreover, to clearly show the relative strength of each helicity amplitude, we list the numerical results for the helicity fraction defined as

$$f_{\lambda_1\lambda_2}(\bar{B}_q^* \to D_q^* V) = \frac{\left|\mathcal{A}_{\lambda_1\lambda_2}(\bar{B}_q^* \to D_q^* V)\right|^2}{\sum_{\lambda_1,\lambda_2}\left|\mathcal{A}_{\lambda_1\lambda_2}(\bar{B}_q^* \to D_q^* V)\right|^2} \tag{32}$$

in Table 2. The following are some discussions.

From Table 2, there is a very clear hierarchy of the branching fractions indicating that $\mathcal{B}(\bar{B}_q^* \to D_q^* \rho^-) > \mathcal{B}(\bar{B}_q^* \to D_q^* K^{*-})$ and $\mathcal{B}(\bar{B}_q^* \to D_q^* D_s^{*-}) > \mathcal{B}(\bar{B}_q^* \to D_q^* D^{*-})$, which is mainly caused by CKM factors $V_{cb}V_{ud} : V_{cb}V_{us} \approx V_{cb}V_{cs} : V_{cb}V_{cd} \approx 1/\lambda$. Meanwhile, $\mathcal{B}(\bar{B}_q^* \to D_q^* D_s^{*-}) > \mathcal{B}(\bar{B}_q^* \to D_q^* \rho^-)$ and $\mathcal{B}(\bar{B}_q^* \to D_q^* D^{*-}) > \mathcal{B}(\bar{B}_q^* \to D_q^* K^{*-})$ because $f_{D_s^*} > f_\rho$ and $f_{D^*} > f_{K^*}$, respectively. The CKM favored $\bar{B}_q^* \to D_q^* \rho^-$ and $D_q^* \bar{D}_s^*$ decays have relatively large branching fractions, $\gtrsim \mathcal{O}(10^{-8})$, and therefore it might be possible to observe them by LHC and Belle-II experiments.

The $\bar{B}^* \to V_L V_L$ (V_L denotes light vector meson) decay modes should have much smaller branching fraction, $< \mathcal{O}(10^{-9})$, because they are suppressed at least by the CKM factor and relatively small form factors. They are generally out of the scope of LHC and Belle-II experiments, and thus are not considered in this study.

The $SU(3)$ flavor symmetry acting on the spectator quark requires that

$$\mathcal{A}(B^{*-} \to D^{*0} V) \approx \mathcal{A}(\bar{B}_d^{*0} \to D^{*+} V) \approx \mathcal{A}(\bar{B}_s^{*0} \to D_s^{*+} V), \tag{33}$$

which implies the relation that

$$\mathcal{B}(B^{*-} \to D^{*0} V) : \mathcal{B}(\bar{B}_d^{*0} \to D^{*+} V) : \mathcal{B}(\bar{B}_s^{*0} \to D_s^{*+} V) \approx \frac{1}{\Gamma_{\rm tot}(B^{*-})} : \frac{1}{\Gamma_{\rm tot}(\bar{B}^{*0})} : \frac{1}{\Gamma_{\rm tot}(\bar{B}_s^{*})}. \tag{34}$$

From Eqs. (28)–(30) and Table 2, it can be easily found that our numerical results agree well with such relation required by the $SU(3)$ flavor symmetry.

• There is also a clear hierarchy of helicity amplitudes for a given $\bar{B}_q^* \to D_q^* V$ decay. The helicity picture for the case of $\lambda_{B^*} = 0$ is similar to the case of $\bar{B}_q \to D_q^* V$ decay [56–58], and the only difference is the helicity of the spectator quark. As shown in Table 3, relative to the $(\lambda_{D^*}, \lambda_V) = (0,0)$ helicity state, the contribution of the $(-,-)$ state, H_{--}, is suppressed, because the b quark has to flip its spin in the interaction. For the contribution of the $(+,+)$ state, besides of the spin flip, it is also suppressed by the $(V-A)$ interaction, because the final quark in the $(V-A)$ interaction appears in the "wrong" helicity. Therefore, the helicity amplitudes, H_{00}, H_{--}, and H_{++}, should satisfy the relation

$$|H_{00}| \quad > |H_{--}| \quad > |H_{++}|. \tag{35}$$

More explicitly, for the case of the light V meson, the re-

Table 3. Helicity diagrams for helicity states of $\bar{B}^* \to V_1 V_2$ decay, (λ_1, λ_2). Initial B^* meson is at rest and appears at the top left diagrams. S(F) denotes that the corresponding contribution of helicity state is suppressed (favored) by $(V-A)$ interaction and/or spin flip. See text for further explanation.

Helicity state	$(0,0)_1$	$(0,0)_2$	$(-,-)$	$(+,+)$
Helicity diagram	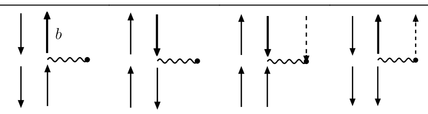			
$(V-A)$/spin flip	F/F	S/F	F/S	S/S
Helicity state	$(-,0)$	$(+,0)$	$(0,-)$	$(0,+)$
Helicity diagram	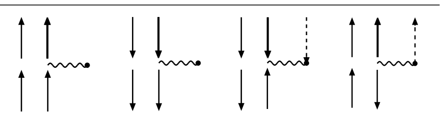			
$(V-A)$/spin flip	F/F	S/F	F/S	S/S

lation $|H_{00}|:|H_{--}|:|H_{++}| \approx 1 : 2m_V/m_{B^*} : 2m_V m_{D^*}/m^2_{B^*}$ expected in the $\bar{B}_q \to D^*_q V_L$ decay [56–58] is also satisfied by the $\bar{B}^*_q \to D^*_q V_L$ decay. For the case of the heavy V meson, the suppression caused by the spin flip is not as strong as the case of light V meson, therefore the f_{00} is relatively small. Our numerical results in Table 2 are consistent with the analyses mentioned above.

Similar analyses can be further applied to the cases $\lambda_{B^*} = -$ and $+$. Hence, it is expected that $|H_{-0}| > |H_{0+}|$ and $|H_{+0}| \gtrsim |H_{0-}|$. However, the later is not satisfied numerically, even though they follow $|H_{+0}|:|H_{0-}| \approx m_{D^*}/m_V$ in form. This is caused by the fact that the main contributions related to $\tilde{V}_1$ and $\tilde{A}_1$ in H_{+0}, Eq. (9), almost completely cancel each other out, because $(\tilde{V}_1 - \tilde{A}_1) \lesssim O(10^{-2})$ is predicted by CLFQM.

After making some comparisons on the helicity states: $(0,0)$ vs. $(-,0)$, $(-,-)$ vs. $(0,-)$ and $(+,+)$ vs. $(0,+)$ in Table 3, we find that their helicity diagrams are the same except for the helicity of the spectator quark, which is trivial for analyzing the suppressions induced by the $(V-A)$ interaction and spin flip. Therefore, it is expected that

$$|H_{-0}| \approx 2|H_{00}|, \quad |H_{0-}| \approx |H_{--}|, \quad |H_{0+}| \approx |H_{++}|. \tag{36}$$

The factor 2 in the first relation is because the vector state $|J, J_z\rangle = |1,0\rangle$ can be expanded in terms of its constituent (anti-)quark 's spin states as $|1,0\rangle = \frac{1}{\sqrt{2}}\left(|\frac{1}{2},-\frac{1}{2}\rangle|\frac{1}{2},\frac{1}{2}\rangle + |\frac{1}{2},\frac{1}{2}\rangle|\frac{1}{2},-\frac{1}{2}\rangle\right)$, in which the first and second terms correspond to the B^* meson, as well as the recoil vector meson, in $(0,0)_1$ and $(0,0)_2$ states (see Table 3), respectively. Meanwhile, for the B^* and recoil vector mesons in the$(-,0)$ helicity state, we have $|1,-1\rangle = |\frac{1}{2},-\frac{1}{2}\rangle|\frac{1}{2},-\frac{1}{2}\rangle$. Therefore, the contribution of $(0,0) \approx (0,0)_1$ helicity state receives an additional factor 1/2 relative to the contribution of the $(-,0)$ state. The effect of such a normalization factor results in a significant difference between the $B^* \to VV$ and $B \to VV$ decay modes, where the former is dominated by the $(-,0)$ state, whereas the latter is dominated by the $(0,0)$ state.

The findings given by Eq. (36) can be easily confirmed by our numerical results listed in Table 2. Taking $\bar{B}^{*0} \to D^{*+}K^{*-}$ decay as an example, we obtain

$$|H_{-0}|:|H_{00}| = 1.93 \text{ vs. } 2, \quad |H_{0-}|:|H_{--}| = 1.03 \text{ vs. } 1,$$
$$|H_{0+}|:|H_{++}| = 0.89 \text{ vs. } 1, \tag{37}$$

where, for the two values in each relation, the former is our numerical result, and the latter is the expectation of Eq. (36).

Combining the findings given above, we can finally conclude the hierarchy of contributions of helicity states as follows:

$$|H_{-0}| \approx 2|H_{00}| \quad > |H_{0-}| \approx |H_{--}| \quad > |H_{0+}| \approx |H_{++}|. \tag{38}$$

4 Summary

In this study, motivated by the experiments of heavy flavor physics at running LHC and SuperKEKB/Belle-II with high-luminosity, the tree-dominated nonleptonic $\bar{B}^*_q \to D^*_q V$ $(q = u, d, s$ and $V = D^{*-}, D^{*-}_s, K^{*-}, \rho^-)$ decays are studied first within the framework of the factorization approach, in which the transition form factors of $\bar{B}^*_q \to D^*_q$ and $\bar{B}^* \to K^*, \rho$ transitions are calculated within the covariant light-front quark model. The helicity amplitudes are calculated and analyzed in detail. These decays are dominated by the $(\lambda_{D^*_q}, \lambda_V) = (-,0)$ helicity state, and the contribution of the $(0,0)$ state is about half of the one of $(-,0)$ state in amplitude. This is obviously different from the B meson decay, which is dominated by the $(0,0)$ state. Moreover, the helicity amplitudes of $\bar{B}^*_q \to D^*_q V$ decays follow a very clear hierarchical structure, given by Eq. (38). The branching fractions are computed, and the effects of CKM factor, $SU(3)$ flavor symmetry and total decay width are discussed in detail. Numerically, the CKM-favored $\bar{B}^*_q \to D^*_q \rho^-$ and $D^*_q D^{*-}_s$ decays have relatively large branching fractions, $\gtrsim O(10^{-8})$, which are expected to be observable in LHC and Belle-II experiments in the future.

Appendix: Form factors of $V' \to V''$ transition in CLFQM

Using the theoretical formalism of the CLFQM detailed in Refs. [53–55], we obtain the form factors of the $V' \to V''$ transition written as

$$\tilde{A}_1(q^2) = \frac{N_c}{16\pi^3}\int dx d^2k_\perp \frac{h'h''}{\bar{x}\hat{N}'_1\hat{N}''_1}(-4)\Big[-2A^{(2)}_1 + \frac{1}{4}(m'^2_1 + m''^2_1 - q^2 + \hat{N}'_1 + \hat{N}''_1) - \frac{1}{2}m'_1 m''_1 + A^{(1)}_1\Big(m^2_2 - \frac{M'^2 + M''^2}{2} + \frac{1}{2}q^2 + m'_1 m''_1 - m'_1 m_2 - m''_1 m_2\Big) + \Big(\frac{1}{D_{V'}} + \frac{1}{D_{V''}}\Big)(m'_1 + m''_1)A^{(2)}_1\Big], \tag{A1}$$

$$\tilde{A}_2(q^2) = \frac{N_c}{16\pi^3}\int dx d^2k_\perp \frac{h'h''}{\bar{x}\hat{N}'_1\hat{N}''_1}4\Big[m'_1 m_2 - \frac{1}{2}m'_1 m''_1 - \frac{1}{4}(m'^2_1 + m''^2_1 - q^2 + \hat{N}'_1 + \hat{N}''_1) + \frac{x}{2}(M'^2 + M''^2 - q^2) - \frac{k_\perp \cdot q_\perp}{2q^2}(M'^2 - M''^2 - q^2) + A^{(2)}_1\frac{M'^2 - M''^2}{q^2} + A^{(1)}_2\Big(m^2_2 - \frac{M'^2 + M''^2}{2} + Z_2 + \frac{1}{2}q^2 + m'_1 m''_1 - m'_1 m_2 - m''_1 m_2\Big) + \Big(\frac{-m'_1 + m''_1 - 2m_2}{D_{V'}} + \frac{-m'_1 + m''_1 + 2m_2}{D_{V''}}\Big)A^{(2)}_1\Big], \tag{A2}$$

$$\tilde{A}_3(q^2)=\frac{N_c}{16\pi^3}\int \mathrm{d}x\mathrm{d}^2k_\perp \frac{h'h''}{\bar{x}\hat{N}_1'\hat{N}_1''}(-4)(M'^2-M''^2)\Big[(A_4^{(2)}+A_1^{(1)}-A_2^{(2)}-A_2^{(1)}) + \frac{m_1'}{D_{V''}}(-A_4^{(2)}-2A_3^{(2)}-A_2^{(2)}+2A_2^{(1)}+2A_1^{(1)}-1)+\frac{m_1''}{D_{V''}}(-A_4^{(2)} + A_2^{(2)}+A_2^{(1)}-A_1^{(1)})+\frac{2m_2}{D_{V''}}(A_3^{(2)}+A_2^{(2)}-A_1^{(1)}) + \frac{2}{D_{V'}D_{V''}}(-A_2^{(3)}-A_1^{(3)}+A_1^{(2)})\Big], \tag{A3}$$

$$\tilde{A}_4(q^2)=\frac{N_c}{16\pi^3}\int \mathrm{d}x\mathrm{d}^2k_\perp \frac{h'h''}{\bar{x}\hat{N}_1'\hat{N}_1''}4(M'^2-M''^2)\Big[(-A_4^{(2)}-A_1^{(1)}+A_2^{(2)}+A_2^{(1)}) + \frac{m_1'}{D_{V'}}(A_4^{(2)}-A_2^{(2)}-A_2^{(1)}+A_1^{(1)})+\frac{m_1''}{D_{V'}}(A_4^{(2)}-2A_3^{(2)}+A_2^{(2)}) + \frac{2m_2}{D_{V'}}(A_3^{(2)}-A_2^{(2)})+\frac{2}{D_{V'}D_{V''}}(A_1^{(3)}-A_2^{(3)})\Big], \tag{A4}$$

$$\tilde{V}_1(q^2)=\frac{N_c}{16\pi^3}\int \mathrm{d}x\mathrm{d}^2k_\perp \frac{h'h''}{\bar{x}\hat{N}_1'\hat{N}_1''}(-1)\Big\{[-16A_1^{(3)}-2f(x,k_\perp,q_\perp) -4x(m_1'+m_1'')m_2]+\frac{4}{D_{V'}}[m_1'(4A_1^{(3)}-A_1^{(2)})+m_1''A_1^{(2)}+4m_2A_1^{(3)}] + \frac{4}{D_{V''}}[m_1'A_1^{(2)}+m_1''(4A_1^{(3)}-A_1^{(2)})+4m_2A_1^{(3)}] + \frac{8}{D_{V'}D_{V''}}f(x,k_\perp,q_\perp)A_1^{(2)}\Big\}, \tag{A5}$$

$$\tilde{V}_2(q^2)=\frac{N_c}{16\pi^3}\int \mathrm{d}x\mathrm{d}^2k_\perp \frac{h'h''}{\bar{x}\hat{N}_1'\hat{N}_1''}\Big\{-16A_2^{(3)}+8A_1^{(2)}-m_1'^2+m_1''^2-2m_2^2-q^2 +2M'^2-2Z_2-\hat{N}_1'+\hat{N}_1''-2m_1'm_1''+4m_1'm_2+4A_2^{(1)}\Big(m_2^2 -\frac{M'^2+M''^2}{2}+\frac{1}{2}q^2+m_1'm_1''-m_1'm_2-m_1''m_2\Big)+4\Big(A_2^{(1)}Z_2 +\frac{M'^2-M''^2}{q^2}A_1^{(2)}\Big)+16\Big(\frac{m_1'+m_2}{D_{V'}}+\frac{m_1''+m_2}{D_{V''}}\Big)A_2^{(3)} +4\Big(\frac{-3m_1'+m''_1-2m_2}{D_{V'}}+\frac{-m_1'-m_1''-2m_2}{D_{V''}}\Big)A_1^{(2)} -\Big(m_2^2-\frac{M'^2+M''^2}{2}+\frac{1}{2}q^2+m_1'm_1''-m_1'm_2-m_1''m_2\Big) \times\frac{16}{D_{V'}D_{V''}}A_2^{(3)}-\frac{16}{D_{V'}D_{V''}}\left[A_2^{(3)}Z_2+\frac{M'^2-M''^2}{3q^2}(A_1^{(2)})^2\right] +(m_1'^2-m_1''^2+2m_2^2+q^2-2M'^2+\hat{N}_1'-\hat{N}_1''+2m'_1m_1'' -4m_1'm_2)\frac{4}{D_{V'}D_{V''}}A_1^{(2)}+\frac{8}{D_{V'}D_{V''}}A_1^{(2)}Z_2\Big\}, \tag{A6}$$

$$\tilde{V}_3(q^2)=\frac{N_c}{16\pi^3}\int \mathrm{d}x\mathrm{d}^2k_\perp \frac{h'h''}{\bar{x}\hat{N}_1'\hat{N}_1''}(M'^2-M''^2)\Big\{8x(A_2^{(2)}-A_4^{(2)}+A_2^{(1)}-A_1^{(1)}) +\frac{4}{D_{V'}}[m_1'(1-2x)(A_2^{(2)}-A_4^{(2)}+A_2^{(1)}-A_1^{(1)})+m_1''(A_2^{(2)}+A_4^{(2)}-2A_3^{(2)}) +m_2x(2A_4^{(2)}-2A_2^{(2)}+A_1^{(1)}-A_2^{(1)})] +\frac{4}{D_{V''}}[m_1'(A_2^{(2)}+2A_3^{(2)}+A_4^{(2)}-2A_2^{(1)}-2A_1^{(1)}+1) +m_1''(1-2x)(A_2^{(2)}-A_4^{(2)}+A_2^{(1)}-A_1^{(1)}) +2m_2(2A_5^{(3)}-2A_3^{(3)}+A_2^{(2)}-3A_3^{(2)}+A_1^{(1)})] -\frac{8}{D_{V'}D_{V''}}(A_2^{(2)}-A_4^{(2)}+A_2^{(1)}-A_1^{(1)})f(x,k_\perp,q_\perp)\Big\}, \tag{A7}$$

$$\tilde{V}_4(q^2)=\frac{N_c}{16\pi^3}\int \mathrm{d}x\mathrm{d}^2k_\perp \frac{h'h''}{\bar{x}\hat{N}_1'\hat{N}_1''}(M''^2-M'^2)\Big\{8(2A_4^{(3)}-2A_6^{(3)}-2A_3^{(2)} +3A_4^{(2)}+A_1^{(1)}-A_2^{(1)}-A_2^{(2)})+4\frac{m_1'}{D_{V'}}(-4A_4^{(3)}+4A_6^{(3)}+4A_3^{(2)}+3A_2^{(2)} -7A_4^{(2)}-3A_1^{(1)}+3A_2^{(1)})+4\frac{m_1''}{D_{V'}}(2A_3^{(2)}-A_4^{(2)}-A_2^{(2)}) +8\frac{m_2}{D_{V'}}(-2A_4^{(3)}+2A_6^{(3)}+A_3^{(2)}+A_2^{(2)}-2A_4^{(2)}) +4\frac{m_1'}{D_{V''}}(1-2A_1^{(1)}-2A_2^{(1)}+A_2^{(2)}+2A_3^{(2)}+A_4^{(2)}) +4\frac{m_1''}{D_{V''}}(-A_1^{(1)}+2A_2^{(1)}+A_2^{(2)}+4A_3^{(2)}+4A_6^{(3)}-4A_4^{(3)}-5A_4^{(2)}) +8\frac{m_2}{D_{V''}}(-A_1^{(1)}+2A_2^{(1)}+A_2^{(2)}+A_3^{(2)}+2A_6^{(3)}-2A_4^{(3)}-4A_4^{(2)}) +\frac{16}{D_{V'}D_{V''}}(-A_3^{(2)}+A_4^{(2)}+A_4^{(3)}-A_6^{(3)})\Big(m_2^2-\frac{M'^2+M''^2}{2} +\frac{1}{2}q^2+m_1'm_1''+m_1'm_2+m_1''m_2\Big)-\frac{8}{D_{V'}D_{V''}}(A_2^{(1)}-3A_4^{(2)} +2A_6^{(3)})Z_2-\frac{4}{D_{V'}D_{V''}}(A_1^{(1)}-A_2^{(1)}-A_2^{(2)}+A_4^{(2)})[2M'^2+(m_{1'}-m_{1''})^2 -2(m_{1'}+m_2)^2-q^2-\hat{N}_{1'}+\hat{N}_{1''}] -\frac{8}{D_{V'}D_{V''}}\left[A_1^{(2)}-6A_1^{(2)}A_2^{(1)}+6A_2^{(1)}A_2^{(3)}-2\frac{(A_1^{(2)})^2}{q^2}\right]\frac{M'^2-M''^2}{q^2}\Big\}, \tag{A8}$$

$$\tilde{V}_5(q^2)=\frac{N_c}{16\pi^3}\int \mathrm{d}x\mathrm{d}^2k_\perp \frac{h'h''}{\bar{x}\hat{N}_1'\hat{N}_1''}(-1)\Big\{16(A_1^{(3)}-A_2^{(3)})+2(\hat{N}_1'+m_1'^2-M'^2 +Z_2+m_2^2-2m_1'm_2)+4(A_2^{(1)}-A_1^{(1)})\Big(\hat{N}_1''+m_1''^2+\frac{M'^2-M''^2-q^2}{2} -m_1'm_1''+m_1'm_2-m_1''m_2\Big)+\frac{4}{D_{V'}}\times\Big[m_1'\Big(4(A_2^{(3)}-A_1^{(3)})+(A_2^{(1)}-A_1^{(1)}) \times(M''^2-\hat{N}_1''-m_1''^2-m_2^2)-(A_2^{(1)}Z_2+\frac{M'^2-M''^2}{q^2}A_1^{(2)})\Big) +m_1''\Big((A_2^{(1)}-A_1^{(1)})(\hat{N}_1'-M'^2+m_1'^2-m_2^2)+(A_2^{(1)}Z_2+\frac{M'^2-M''^2}{q^2}A_1^{(2)})\Big) +m_2\Big(4(A_2^{(3)}-A_1^{(3)})+(A_2^{(1)}-A_1^{(1)})(-\hat{N}_1'-\hat{N}_1''-m_1'^2-m_1''^2-q_\perp^2 +2m_1'm_1'')\Big)\Big]+\frac{4}{D_{V''}}\Big[2m_1'A_1^{(2)}+4m_1''4(A_2^{(3)}-A_1^{(3)})+m_2\Big(4(A_2^{(3)}-A_1^{(3)}) -2A_1^{(2)}\Big)\Big]+\frac{16}{D_{V'}D_{V''}}\Big[(A_2^{(3)}-A_1^{(3)})\Big(-m_1'm_1''-m_2^2-m_1'm_2-m_1''m_2 -\frac{M'^2-M''^2+q^2}{2}+M'^2\Big)-A_2^{(3)}Z_2-\frac{M'^2-M''^2}{3q^2}(A_1^{(2)})^2\Big]\Big\}, \tag{A9}$$

$$\tilde{V}_6(q^2)=\frac{N_c}{16\pi^3}\int \mathrm{d}x\mathrm{d}^2k_\perp \frac{h'h''}{\bar{x}\hat{N}_1'\hat{N}_1''}\Big\{16(A_1^{(2)}-A_1^{(3)}-A_2^{(3)})+2(-2m_1'^2 -m_1''^2-m_2^2+q^2+M'^2-Z_2-2\hat{N}_1'-\hat{N}_1''+2m_1'm_1''+2m_1'm_2) +4(A_2^{(1)}+A_1^{(1)})\Big(m_1'^2+\frac{M'^2-M''^2}{2}+\hat{N}_1'-\frac{1}{2}q^2-m_1'm_1'' -m_1'm_2-m_1''m_2\Big)+\frac{16}{D_{V'}}\Big[(m_1'+m_2)(A_1^{(3)}+A_2^{(3)})-\Big(m_1' +\frac{1}{2}m_1''+\frac{1}{2}m_2\Big)A_1^{(2)}\Big]+4\frac{m_1'}{D_{V''}}(-m_1''^2-m_2^2+M''^2-Z_2-\hat{N}_1'') +\frac{16}{D_{V''}}(m_1''+m_2)(A_1^{(3)}+A_2^{(3)}-A_1^{(2)})+\frac{4}{D_{V''}}[m_1''(m_1'^2+m_2^2-M'^2 +Z_2+\hat{N}_1')+m_2(m_1'^2+m_1''^2-q^2+\hat{N}_1'+\hat{N}_1''-2m_1'm_1'')] +\frac{4}{D_{V''}}(A_1^{(1)}+A_2^{(1)})[m_1'(m_1''^2+m_2^2-M''^2+\hat{N}_1'')+m_1''(-m_1'^2-m_2^2$$

$$+M'^2-\hat{N}'_1)+m_2(-m_1'^2-m_1''^2+q^2-\hat{N}'_1-\hat{N}''_1+2m'_1m''_1)]$$
$$+\frac{4}{D_{V''}}(m'_1-m''_1)\left(A_2^{(1)}Z_2+\frac{M'^2-M''^2}{q^2}A_1^{(2)}\right)-\frac{16}{D_{V'}D_{V''}}(A_1^{(3)}+A_2^{(3)}$$
$$-A_1^{(2)})\left(m_2^2-\frac{M'^2+M''^2}{2}+\frac{1}{2}q^2+m'_1m''_1+m'_1m_2+m''_1m_2\right)$$
$$-\frac{16}{D_{V'}D_{V''}}\left[A_2^{(3)}Z_2+\frac{M'^2-M''^2}{3q^2}(A_1^{(2)})^2-A_1^{(2)}Z_2\right]\Bigg\},\qquad (A10)$$

where $f(x,k_\perp,q_\perp)=\frac{x^2}{\bar{x}}m_2^2+\frac{1}{\bar{x}}k_\perp^2-k_\perp\cdot q_\perp+\bar{x}m'_1m''_1-x(m'_1m_2+m''_1m_2)$ and $D_{V'(\prime\prime)}=M_0^{\prime(\prime\prime)}+m_1^{\prime(\prime\prime)}+m_2$ is the factor appearing in the vertex operator. Here, we use the same notation and convention as Refs. [53–55], and the explicit forms of Z_2, $h^{\prime(\prime\prime)}/\hat{N}_1^{\prime(\prime\prime)}$ and $A_i^{(j)}$ functions can be easily found therein.

References

1 R. Aaij et al (LHCb Collaboration), Eur. Phys. J. C, **73**(4): 2373 (2013)
2 T. Abe et al (Belle-II Collaboration), arXiv:1011.0352 [physics.ins-det]
3 M. Tanabashi et al (Particle Data Group), Phys. Rev. D, **98**(3): 030001 (2018)
4 N. Isgur and M. B. Wise, Phys. Rev. Lett., **66**: 1130 (1991)
5 S. Godfrey and R. Kokoski, Phys. Rev. D, **43**: 1679 (1991)
6 E. J. Eichten, C. T. Hill and C. Quigg, Phys. Rev. Lett., **71**: 4116 (1993)
7 D. Ebert, V. O. Galkin, and R. N. Faustov, Phys. Rev. D, **57:** (1998) 5663 Erratum: [Phys. Rev. D, **59:** (1999) 019902]
8 R. Aaij et al (LHCb Collaboration), Int. J. Mod. Phys. A, **30**(07): 1530022 (2015)
9 Q. Chang, P. P. Li, X. H. Hu et al, Int. J. Mod. Phys. A, **30**(27): 1550162 (2015)
10 R. Aaij et al (LHCb Collaboration), Phys. Lett. B, **694**: 209 (2010)
11 B. Grinstein and J. Martin Camalich, Phys. Rev. Lett., **116**(14): 141801 (2016)
12 H. K. Sun and M. Z. Yang, Phys. Rev. D, **99**(9): 093002 (2019)
13 G. Z. Xu, Y. Qiu, C. P. Shen et al, Eur. Phys. J. C, **76**(11): 583 (2016)
14 J. Saini, D. Kumar, S. Gangal et al, arXiv:1905.03933 [hep-ph].
15 S. Kumbhakar and J. Saini, Eur. Phys. J. C, **79**(5): 394 (2019)
16 D. Banerjee, P. Maji, and S. Sahoo, Int. J. Mod. Phys. A, **32**(14): 1750075 (2017)
17 S. Sahoo and R. Mohanta, Springer Proc. Phys., **203**: 321 (2018)
18 Z. G. Wang, Commun. Theor. Phys., **61**(1): 81 (2014)
19 K. Zeynali, V. Bashiry, and F. Zolfagharpour, Eur. Phys. J. A, **50**: 127 (2014)
20 V. Bashiry, Adv. High Energy Phys., **2014**: 503049 (2014)
21 Q. Chang, J. Zhu, X. L. Wang et al, Nucl. Phys. B, **909**: 921 (2016)
22 T. Wang, Y. Jiang, T. Zhou et al, J. Phys. G, **45**(11): 115001 (2018)
23 Q. Chang, J. Zhu, N. Wang et al, Adv. High Energy Phys., **2018**: 7231354 (2018)
24 Q. Chang, X. Hu, J. Sun et al, Adv. High Energy Phys., **2015**: 767523 (2015)
25 J. Sun, H. Li, Y. Yang et al, J. Phys. G, **44**(7): 075007 (2017)
26 Q. Chang, X. Hu, Z. Chang et al, Adv. High Energy Phys., **2016**: 3863725 (2016)
27 Q. Chang, L. X. Chen, Y. Y. Zhang et al, Eur. Phys. J. C, **76**(10): 523 (2016)
28 G. Buchalla, A. J. Buras, and M. E. Lautenbacher, Rev. Mod. Phys., **68**: 1125 (1996)
29 A. J. Buras, hep-ph/9806471
30 D. Fakirov and B. Stech, Nucl. Phys. B, **133**: 315 (1978)
31 N. Cabibbo and L. Maiani, Phys. Lett. B, **73** (1978) 418 Erratum: [Phys. Lett. B, **76** (1978) 663]
32 M. Bauer and B. Stech, Phys. Lett. B, **152**: 380 (1985)
33 M. Wirbel, B. Stech, and M. Bauer, Z. Phys. C, **29**: 637 (1985)
34 M. Bauer, B. Stech, and M. Wirbel, Z. Phys. C, **34**: 103 (1987)
35 J. D. Bjorken, Nucl. Phys. Proc. Suppl., **11**: 325 (1989)
36 P. Jain, B. Pire and J. P. Ralston, Phys. Rept., **271**: 67 (1996)
37 M. Beneke, G. Buchalla, M. Neubert et al, Phys. Rev. Lett., **83**: 1914 (1999)
38 M. Beneke, G. Buchalla, M. Neubert et al, Nucl. Phys. B, **591**: 313 (2000)
39 T. Huber, S. Krankl, and X. Q. Li, JHEP, **1609**: 112 (2016)
40 Y. M. Wang, H. Zou, Z. T. Wei et al, Eur. Phys. J. C, **54**: 107 (2008)
41 V. Lubicz, A. Melis, and S. Simula, PoS LATTICE, **2016**: 291 (2017)
42 A. Bharucha, D. M. Straub, and R. Zwicky, JHEP, **1608**: 098 (2016)
43 V. M. Braun et al, JHEP, **1704**: 082 (2017)
44 J. L. Goity and W. Roberts, Phys. Rev. D, **64**: 094007 (2001)
45 D. Ebert, R. N. Faustov, and V. O. Galkin, Phys. Lett. B, **537**: 241 (2002)
46 S. L. Zhu, W. Y. P. Hwang, and Z. s. Yang, Mod. Phys. Lett. A, **12**: 3027 (1997)
47 T. M. Aliev, D. A. Demir, E. Iltan et al, Phys. Rev. D, **54**: 857 (1996)
48 P. Colangelo, F. De Fazio, and G. Nardulli, Phys. Lett. B, **316**: 555 (1993)
49 H. M. Choi, Phys. Rev. D, **75**: 073016 (2007)
50 C. Y. Cheung and C. W. Hwang, JHEP, **1404**: 177 (2014)
51 Q. Chang, X. N. Li, X. Q. Li et al, Phys. Rev. D, **98**(11): 114018 (2018)
52 Q. Chang, X. N. Li, and L. T. Wang, Eur. Phys. J. C, **79**(5): 422 (2019)
53 W. Jaus, Phys. Rev. D, **60**: 054026 (1999)
54 W. Jaus, Phys. Rev. D, **67**: 094010 (2003)
55 H. Y. Cheng, C. K. Chua, and C. W. Hwang, Phys. Rev. D, **69**: 074025 (2004)
56 A. Ali, J. G. Korner, G. Kramer et al, Z. Phys. C, **1**: 269 (1979)
57 J. G. Korner and G. R. Goldstein, Phys. Lett. B, **89**: 105 (1979)
58 A. L. Kagan, Phys. Lett. B, **601**: 151 (2004)